©Journal of Sports Science and Medicine (2025) **24,** 801-812
http://www.jssm.org DOI: https://doi.org/10.52082/jssm.2025.801

Research article

Coordination Patterns of The Swimming Start: A Comparative Study Between Elite and Sub-Elite Swimmers

Yi Lin [1], Shudong Li [1]✉, Luqi Yang [1], Zhanyi Zhou [1], Julien S. Baker [2] and Yaodong Gu [1]✉
[1] Faculty of Sports Science, Ningbo University, Ningbo, China
[2] Department of Sport and Physical Education, Hong Kong Baptist University, Hong Kong, China

Abstract
This study investigated upper-lower body coordination during the swimming start. Coupling angle mapping was applied to assess segmental dominance, coupling angle, and coupling angle variability across four dive-start phases in elite and sub-elite swimmers. Data were collected from twenty swimmers (ten elite and ten sub-elite), based on their three fastest maximal-effort dive starts. The continuous entry movement from air to water was captured in detail using a high-speed multi-camera system positioned above and below the water. Results demonstrated that coordination patterns varied across the four phases, with high similarity when the thigh dominated, such as during the flight phase. Notably, coordination during the on-block phase differed significantly prior to hand-off. Elite swimmers exhibited greater trunk dominance in the entry phase, facilitating a more horizontal dive-in, whereas sub-elite swimmers showed trunk dominance later, during the transition phase. In conclusion, the time required to reach a specific distance or phase does not necessarily indicate superior start performance. Swimmers must balance drag minimization during the dive-in trajectory with rapid entry to initiate stroking. All swimmers maintained a streamlined posture and predominantly employed thigh-dominant strategies, while variations in trunk-dominant coordination were observed during entry and transition phases. Occasional high coupling angle variability in elite swimmers may reflect individualized coordination strategies. These findings highlight the importance of individualised training to optimize start performance.

Key words: Coordination pattern, Biomechanics, Swimming start, Coupling angle mapping, Segmental dominance.

Introduction

The swimming start is crucial in competitive swimming, as the maximum horizontal velocity during the start can reach approximately 4m/s, more than twice the velocity of free swimming(Kiuchi et al., 2010). Trembley and Fielder(Trembley and Fielder, 2001) reported that optimal swim-starts are achieved through a quick block push, a long aerial distance, and a clean entry with powerful underwater propulsion. Unlike track and field, where athletes must accelerate from zero to full speed, swimmers can enter the water faster than their average swimming speed. Studies have shown that the start to 15m accounts for 0.8%-26.1% of the total race time, highlighting the importance of a strong start (Arellano et al., 1996; Cossor and Mason, 2001; Mason et al., 2007; Seifert et al., 2010a; Thayer and Hay, 1984; Vantorre et al., 2010a). As competition rules evolve, so does the swimming start technique, with increasing emphasis on its importance in training to assess athlete performance and technique(Slawson et al., 2013; Takeda et al., 2012; Tor et al., 2015).

The dive start was typically divided into block phase, flight phase, entry phases and glide phase(Vantorre et al., 2014). Swimmers often use different strategies in the flight and entry phases(Vantorre et al., 2010b). The "flat" start, with a lower velocity and flat aerial trajectory, aims for a quick entry and earlier stroking. In contrast, the "pike" style involves a longer push-off and shorter entry distance, creating a smaller hole to minimize aquatic resistance, resulting in a longer aerial trajectory (Vantorre et al., 2014). Elite swimmers also use distinct start styles, such as the Volkov start, named after the swimmer who pioneered the arm swing during the block and flight phases (e.g., Caeleb Dressel), and the flight style, where the arms are positioned in front of the head (e.g., Sun Yang)(Vantorre et al., 2014). Defining the best dive start remains a challenge.

However, according to constraint-led approach(Bartlett et al., 2007; Powell et al., 2021; Seifert et al., 2010a) the answer may not be best start style, but the best strategies suit the specific swimmer according his/her strength and conditioning, event, and skills level. The competitive swimming research about dive start using underwater cameras were mainly based on the data direct from biomechanical measurements, such as time, joint angle, distance, force, and velocity(Tor et al., 2015). However, these data seem not evident to provide the coordination pattern required for swimming dive start. Compared to traditional biomechanical measurement, the quantified coordination pattern would be more event-specific and individualised. Needham et al. (2020) proposed a method for quantifying movement coordination between two segments, calculating coupling angle (CA) based on the angle-angle data of two interested segments.

Biomechanical feedback is essential for athletes, especially after identifying their optimal coordination pattern, offering new insights into swimming performance (Glazier, 2021; Turvey et al., 1978). From the perspective of dynamical systems theory(DST), which conceptualizes movement coordination as emerging from the interaction of multiple system components (i.e., neural, muscular, and environmental constraints), Intertrial variability plays an important role in facilitating transition from one coordination patterns of coordination to another. (Bartlett et al., 2007; Gleim and McHugh, 1997; Gao et al., 2025). This variability is not only an error but also reflects the musculoskeletal system's adaptability to external disturbances,

Received: 09 August 2023 / Accepted: 12 September 2025 / Published (online): 01 December 2025

enhancing performance (Bartlett et al., 2007). Coordination pattern in swimming has been studied since Chollet et al. (2000), who introduced the index of coordination (IdC) to quantify arm movement coordination in swimmers. Their research demonstrated that swimmers adjust arm coordination based on swimming velocity and skill level(Chollet et al., 2000). Seifert et al.(2007) studied arm-to-leg coordination in butterfly stroke(Seifert et al., 2007). while Seifert et al. (2011) explored coordination variability in breaststroke across different skill levels(Seifert et al., 2011). Guignard et al. (2017) focused on quantifying the inter-segmental coordination of the upper limbs in front crawl using the coupling angle.

The coupling angle (CA) may serve as a valuable tool for comparing and analysing different swimming start techniques, offering a more comprehensive understanding of the biomechanics involved and enabling optimization of start techniques based on individual characteristics. This study aims to explore the movement coordination patterns between the trunk and thigh segments during the swimming dive start in elite and sub-elite swimmers, using coupling angle mapping (CAM). We also examine inter-data point range of motion (IDP-ROM), coupling angle variability (CAV), and phase-specific timing (i.e., on-block, flight, entry, and transition) to distinguish coordination patterns across these phases. We hypothesize that the thigh dominant pattern will predominate during most of the dive-in phases, but the distribution of segmental dominance patterns will differ between elite and sub-elite swimmers.

Methods

Participants

Twenty-four male swimmers initially volunteered to participate in this study, including 12 national/international-level (elite) athletes and 12 regional-level (sub-elite) athletes from Zhejiang Province, China. Following Matúš et al(2021), the time to cover 5 m from the starting signal was used as an inclusion criterion for start performance. Based on this criterion, four swimmers were excluded (two elite athletes with slower start times and two sub-elite athletes with faster start times). The final sample comprised 20 swimmers (elite: n = 10; sub-elite: n = 10) (Table 1).

All athletes followed the same training schedule, relaxation therapy, diet, and living environment during the experiment. Participants were in healthy physical condition, with no musculoskeletal injuries or related diseases within the previous six months, and reported no muscle soreness or fatigue on the day of testing. All tests were completed within a single day. Prior to data collection, participants were fully informed of the study procedures, potential risks, and benefits, and provided written informed consent. The study was conducted in accordance with the Declaration of Helsinki and approved by the Ethics Committee of Ningbo University (RAGH20220815).

Experimental Protocol and Procedures

Four Zcam E2 underwater cameras (Zcam E2, CHN) were used to capture video at a sampling frequency of 60Hz. Three cameras were positioned along the edge of the pool at distances of 2.5m, 7.5m, and 12.5m from the starting block. The fourth camera was placed on the poolside, 2.5m from the starting block, to capture aerial views of the starting phase. The cameras were synchronized using the computer's synchronization function to ensure temporal alignment of the video data (Figure 1). To ensure accurate data integration, a custom-designed calibration device was combined with a machine learning-based algorithm to automatically merge the video footage from the four cameras without visible seams.

The test was repeated five times for each participant following a 15-minute warm-up, with a minimum rest interval of 10 minutes between each test to ensure full physical recovery for the swimmers(Slawson et al., 2013; Takeda et al., 2012). During the tests, the coach observed and guided the swimmers' starting movements to meet the test requirements. Finally, the best three out of five trials were selected as the final experimental data for analysis.

Table 1. Mean (± SD) values of main characteristics of the swimmers.

Groups	Sample size	Age	Weight (kg)	Height (cm)	% of WR	FINA points
Elite	10	19.8 ± 2.5	80.6 ± 5.6	186 ± 9.7	90.4 ± 3.3	924 ± 15
Sub-elite	10	18.6 ± 1.4	75.4 ± 6.2	180 ± 6.1	80.2 ± 2.4	810 ± 11

SD = standard deviation; WR = World Record; FINA = Fédération Internationale de Natation (International Swimming Federation).

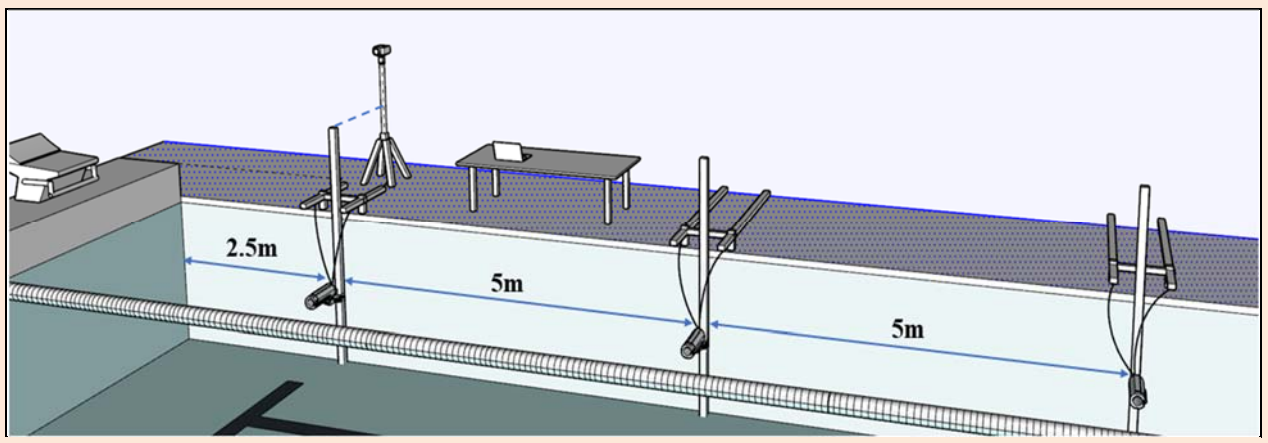

Figure 1. Equipment layout diagram regarding camera set-up.

The Motion videos captured during the tests were calibrated and analysed using the Kinovea software to determine the trunk and thigh angles relative to the horizontal (Karpiński et al., 2020). The software's automatic tracking feature was used, and the Root Mean Squared Error (RMSE) was calculated to compare with the manual digitalization. The intra-class correlation (ICC) was employed to assess the reliability and consistency of angle tracking between three experienced researchers.

A custom-made aluminium rectangular calibration frame (0.8m*3.3m) with a triangular base was placed at the intersection of every two cameras to merge the four separate videos into one cohesive video. The calibration frame centre was placed aligned with the centre black line at the bottom of the swimming pool. Distance calibration in the sagittal plane was performed using two marks on the bottom of the pool: one at five meters from the wall and another at the 15-meter mark along the black line on the pool's bottom. The length of the calibration frame was also used to verify the accuracy of the distance calibration.

Coupling angle and coupling angle mapping

Needham et al. (2020) proposed a method to quantify movement coordination between two segments(Needham et al., 2020),by calculating coupling angles (CA) based on the angle-angle data. Coupling angle mapping (CAM) was used to visualise these patterns and the direction of segmental rotation by different colours (Needham et al., 2020). CAM overcomes the limitations of traditional group data by providing individual coordination profiles and variability. This method offers advantages for coaching and clinical management by revealing participant-specific coordination patterns. Unlike the modified vector coding approach, which can be problematic when overlaying multiple trials, CAM enables the examination of entire datasets and comparison across participants and conditions using colour bins. By mapping segment coupling, variability, and dominance, CAM supports existing data analysis techniques such as coordination profiling and single-subject analysis.

The angle between trunk and horizontal plane (proximal segmental angle) and the angle between thigh and horizontal plane (distal segmental angle) were used to draw the angle-angle diagram (Figure 2). An angle-angle diagram is a functional diagram of one angle to another that provides a quantitative description of the pattern of coordination between body segments in motion(Hershler and Milner, 1980; Pau et al., 2022). However, due to subtle changes in segmental orientation, fixed angles are not allowed for detailed observation of coordination. Therefore, the nonlinear equation is used to calculate the vector direction between adjacent data points in vector coding, which provides a quantitative measurement for the shape of angle-angle graph(Needham et al., 2015). The vector direction can range from 0° to 360°, and this circular variable is called the coupling angle. The coupling angle can be divided to different parts corresponding to specific coordination pattern, as shown in Figure 3. Different colour partitions represent distinct coordination patterns, which reflect body movements and adjustments during different phases of the analysed activity(Needham et al., 2020).

As for coordination pattern of swimming dive start, for instance, the red bins with coupling angle from 0°- 90° (both dark (0°- 45°) and light red (45°-90°) in figure 3 and 4) showed in on-block phase which represents both segmental angles of the trunk and thigh increasing (+/+) i.e., a back shift of the centre of mass while hands grabbing the block. In transition phase, the red bins (in Figure3 and Figure 7) may represents a gradual alignment of the body parallel to the pool bottom after entering the water.

Similarly, the blue bins with coupling angle from 90°- 180° represent the decreasing of trunk segmental angle and the increasing of the thigh segmental angle (-/+). The green bins with coupling angle from 180° - 270° represent the decreasing of trunk segmental angle and the decreasing of the thigh segmental angle (-/-). The purple bins with coupling angle from 270°-360°mean the decreasing of trunk segmental angle and the increasing of the thigh segmental angle (+/-).

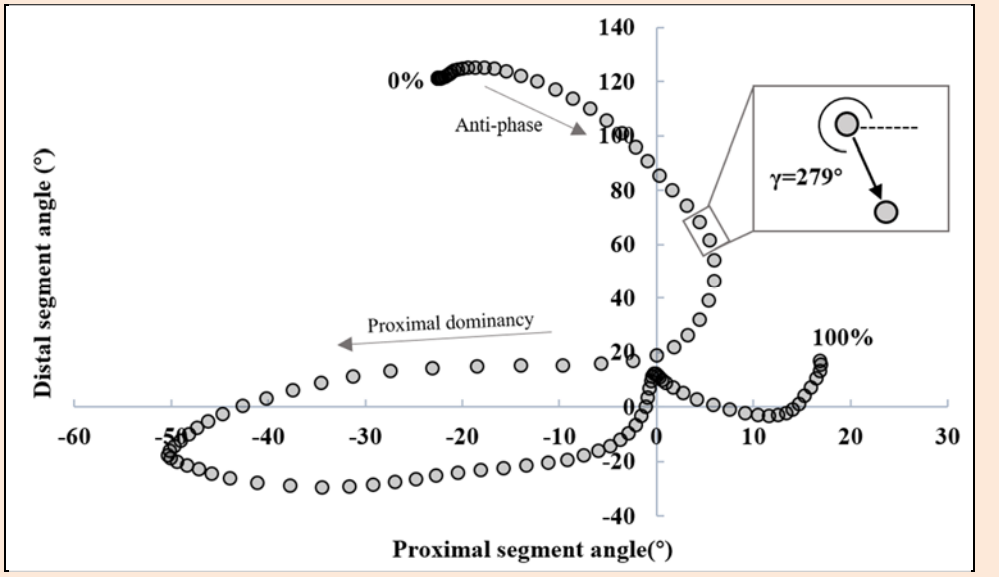

Figure 2. Angle–angle diagram of a swimmer's start. The proximal segment corresponds to the trunk, and the distal segment corresponds to the thigh.

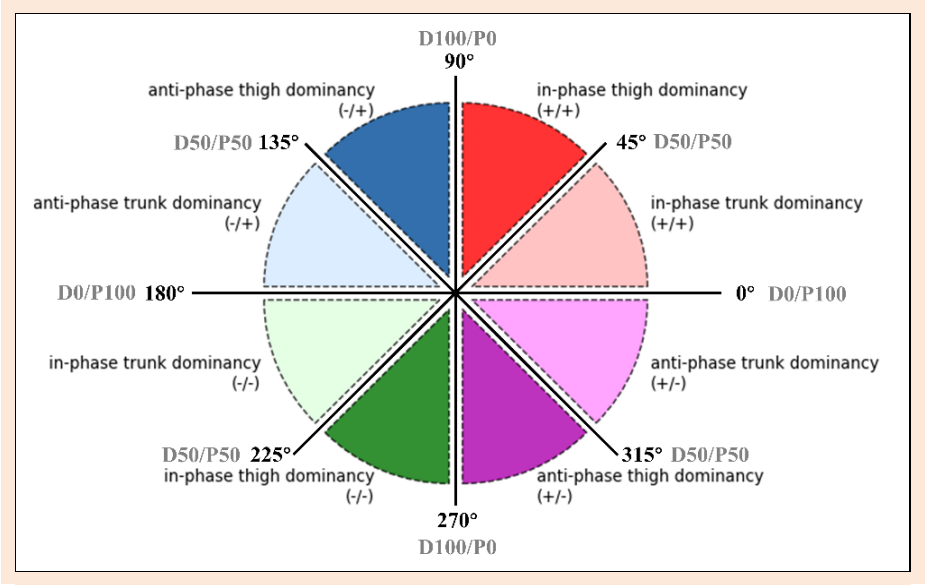

Figure 3. A classification of coordination patterns based on coupling angles. Different colour partitions represent different coordination patterns (black), and segment dominance (grey) is marked around the circumference of the disk graph (D = distal, P = proximal).

Within each colour bin, the dark colour in all colours bin means the segmental angle change of thigh is larger than the trunk between the time interval of two data points (i.e., thigh dominance). While, the trunk dominances are in light colours which closes to x-axis in Figure 3.

Coupling angle ($\boldsymbol{\gamma_i}$) according to the formula based on proximal segmental angle ($\boldsymbol{\theta_{(Pi)}}$,$\boldsymbol{\theta_{(Pi+1)}}$) and distal segmental angle ($\boldsymbol{\theta_{(Di)}}$,$\boldsymbol{\theta_{(Di+1)}}$) is calculated, and the formula is as follows:

$$\boldsymbol{\gamma_i} = \mathbf{Atan}\left(\frac{\theta_{(Di+1)}-\theta_{(Di)}}{\theta_{(Pi+1)}-\theta_{(Pi)}}\right)\cdot\frac{180}{\pi} \quad \text{if } \theta_{(Pi+1)} - \theta_{(Pi)} > 0 \qquad (1)$$

$$\boldsymbol{\gamma_i} = \mathbf{Atan}\left(\frac{\theta_{(Di+1)}-\theta_{(Di)}}{\theta_{(Pi+1)}-\theta_{(Pi)}}\right)\cdot\frac{180}{\pi} + 180 \quad \text{if } \theta_{(Pi+1)} - \theta_{(Pi)} < 0 \qquad (2)$$

($\boldsymbol{\gamma_i}$) is a special value when:

$$\gamma_i = \begin{cases} \gamma_i = 90 & \theta_{(Pi+1)} - \theta_{(Pi)} = 0 \text{ and } \theta_{(Di+1)} - \theta_{(Di)} > 0 \\ \gamma_i = -90 & \theta_{(Pi+1)} - \theta_{(Pi)} = 0 \text{ and } \theta_{(Di+1)} - \theta_{(Di)} < 0 \\ \gamma_i = -180 & \theta_{(Pi+1)} - \theta_{(Pi)} < 0 \text{ and } \theta_{(Di+1)} - \theta_{(Di)} = 0 \\ \gamma_i = Undefined & \theta_{(Pi+1)} - \theta_{(Pi)} = 0 \text{ and } \theta_{(Di+1)} - \theta_{(Di)} = 0 \end{cases} \qquad (3)$$

The coupling angle (γ_i) is normalised to a value between 0° and 360° according to equation (4):

$$\boldsymbol{\gamma_i} = \begin{cases} \boldsymbol{\gamma_i} + 360 & \boldsymbol{\gamma_i} < 0 \\ \boldsymbol{\gamma_i} & \boldsymbol{\gamma_i} \geq 0 \end{cases} \qquad (4)$$

Coupling angle data is classified into one of four coordination patterns: “in-phase proximal segment dominant”, “in-phase distal segment dominant”, “anti-phase proximal segment dominant”, and “anti-phase distal segment dominant”. In-phase coordination refers to two segments rotating in the same direction, while anti-phase coordination refers to two segments rotating in opposite directions. Each quadrant of the unit circle represents 100 gradients, and converting coupling angles into gradients provides the percentage of proximal or distal segment advantage (e.g. 9° is 10 gradients, 18° is 20 gradients, and 27° is 30 gradients). Segmental dominance means that one of the proximal or distal segments has a larger angle change at each instant of the motion cycle (e.g. 50 gradients when the coupling angle is 45°, thus equal to 0.5 Seg.dom(minimum value of y-axis) in Figure 4, Figure 5, Figure 6, and Figure 7, indicating that the angular rotation of the proximal and distal segments contributes equally to the change in relative angle).

The coupling angle for each phase of the start (on-block, flight, entry, and transition) was plotted using the "coupling angle mapping" method(Needham et al., 2018; Needham et al., 2020). Thes colour code (following Figure 3) of histogram in result figures (Figure 4, Figure 5, Figure 6 and Figure 7) was used to visualize the instantons changes of coordination pattern. The height of histogram quantifies the dominance rate converting from the coupling angle in corresponding colour bins (see grey number in Figure 3). Small amplitude movements may introduce errors in the histogram by using vector coding technique. To address this, the "inter-data point range of motion" (IDP-ROM) of the main segment(Needham et al., 2018; Needham et al., 2020) was used to assess motion amplitude between segments and correct errors caused by small amplitude shaking.

Coupling angle variability

Due to the directional nature of coupling angle, the variability was calculated based on the average horizontal ($\overline{\boldsymbol{X_i}}$) and vertical ($\overline{\boldsymbol{Y_i}}$) evaluated from the coupling angle ($\boldsymbol{\gamma_i}$) at each moment across a number of experiments (n) (Batschelet, 1981), formula is as follows:

$$\overline{X_i} = \frac{1}{n}\sum_{i=1}^{n}\cos\gamma_i \qquad (5)$$

$$\overline{Y_i} = \frac{1}{n}\sum_{i=1}^{n}\sin\gamma_i \qquad (6)$$

The following formula is used to standardize the average coupling angle ($\overline{\boldsymbol{\gamma_i}}$) as a value between 0 ° to 360 °:

$$\overline{\gamma}_i = \begin{cases} \text{Atan}\left(\frac{\overline{Y}_i}{\overline{X}_i}\right)\cdot\frac{180}{\pi} & if\ \overline{X}_i > 0,\ \overline{Y}_i > 0 \\ \text{Atan}\left(\frac{\overline{Y}_i}{\overline{X}_i}\right)\cdot\frac{180}{\pi} + 180 & if\ \overline{X}_i < 0 \\ \text{Atan}\left(\frac{\overline{Y}_i}{\overline{X}_i}\right)\cdot\frac{180}{\pi} + 360 & if\ \overline{X}_i > 0,\ \overline{Y}_i < 0 \\ 90 & if\ \overline{X}_i = 0,\ \overline{Y}_i > 0 \\ -90 & if\ \overline{X}_i = 0,\ \overline{Y}_i < 0 \\ undefined & if\ \overline{X}_i = 0,\ \overline{Y}_i = 0 \end{cases} \quad (7)$$

Average coupling angle ($\overline{\gamma}_i$) length is calculated according to the following formula:

$$\overline{\gamma}_i = \sqrt{\overline{X}_i^2 + \overline{Y}_i^2} \quad (8)$$

Coupling angle variability (CAV_i) is calculated according to the following formula:

$$CAV_i = \sqrt{2\cdot(1-\overline{\gamma}_i)}\cdot\frac{180}{\pi} \quad (9)$$

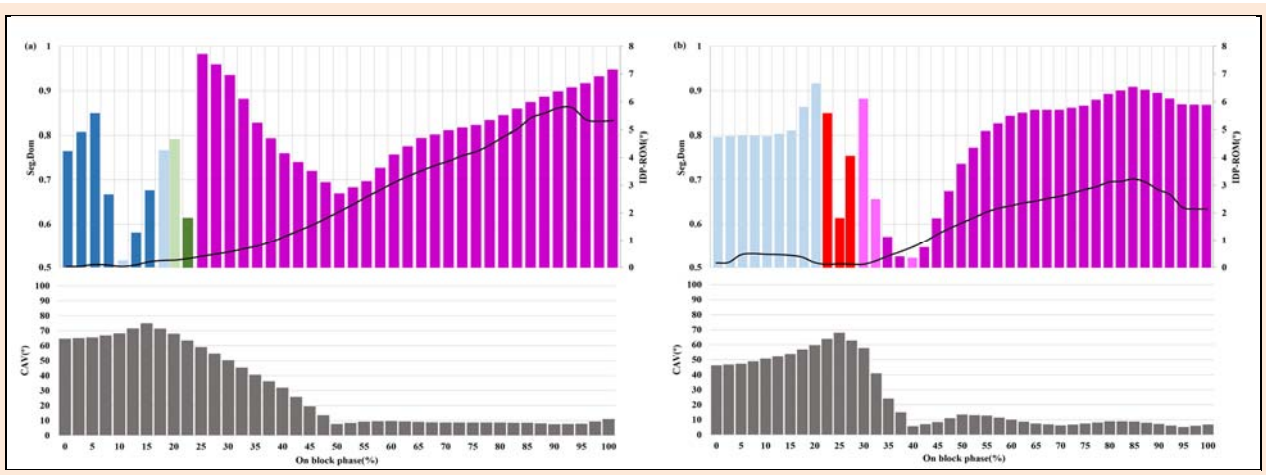

Figure 4. Coupling angle mapping (CAM), segmental dominance (Seg.Dom), IDP-ROM and coupling angle variation profiling representing mean elite (a) and sub-elite (b) trunk-thigh coordination during on block phase (See Figure. 3 for colour-scale legend).

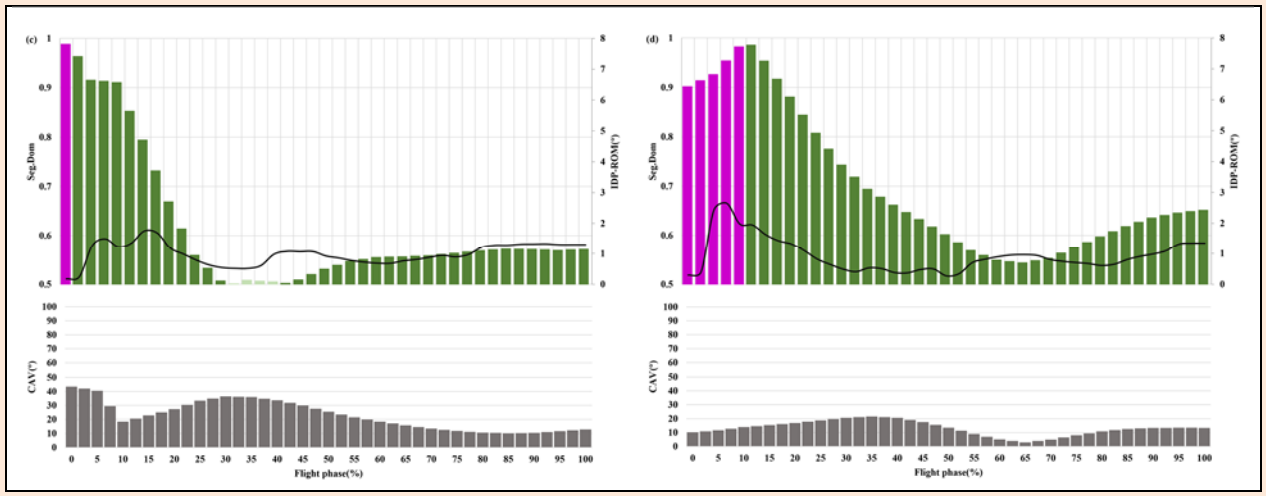

Figure 5. Coupling angle mapping (CAM), segmental dominance (Seg.Dom), Inter-data point range of motion (IDP-ROM) and coupling angle variation(CAV) profiling representing mean elite (c) and sub-elite (d) trunk-thigh coordination during flight phase (See Figure. 3 for colour-scale legend).

Statistical analysis

The resulting data is then imported into Excel for further data analysis and processing. Finally, the coupling angle, coupling angle variability and time were obtained, and the whole start was divided into four phases(Vantorre et al., 2010b): 1. on-block phase: from starting signal to one frame before the front foot off the block; 2. flight phase: from first frame when the front foot leaves the block to one frame before the hand touching the water; 3. entry phase: the phase from the hand touching the water to the whole body is completely immersed in the water; 4. transition phase: from one frame after foot toe entry to one frame before the foot initiates the downbeat kicking. The timing function of Kinovea was used to calculate the time of the four phases, and the difference of the time for different athletes in each phase was analysed statistically.

The resulting data were imported into Excel for further analysis and processing. The CA, CAV, CAM, and time for each phase were then calculated, and the entire dive start was divided into four phases(Vantorre et al.,

2010b): 1) on-block phase: from the start until the front foot leaves the block; 2) flight phase: from when the front foot leaves the block until the hands enter the water; 3) entry phase: from when the hands touch the water until the body is fully submerged; 4) transition phase: from the moment the toes of the foot enter the water until just before the foot initiates the downbeat kicking. Phase durations were determined using the timing function of Kinovea, and statistical analyses were performed to examine differences across athletes.

Statistical analysis was conducted using IBM SPSS Statistics 19 (SPSS Inc, Chicago, IL, USA). The normality of the data was assessed using the Shapiro–Wilk test. Differences in time between elite and sub-elite athletes were analysed using an independent samples t-test, with the significance level set at 0.05. Cohen's d was calculated to determine the effect size of the mean differences. Effect sizes were categorized as trivial (<0.2), small (≥0.2 and <0.5), moderate (≥0.5 and <0.8), or large (≥0.8)(Cohen, 1988).

To assess the validity of the automatic tracking in Kinovea, the Root Mean Square Error (RMSE) between manual and automatic tracking was calculated as a tracking error indicator. Intra-class correlation (ICC) was used to evaluate the consistency between different operators. Reliability was classified as very high (ICC > 0.90), high (0.70 < ICC < 0.89), or moderate (0.50 < ICC < 0.69)(Shrout and Fleiss, 1979).

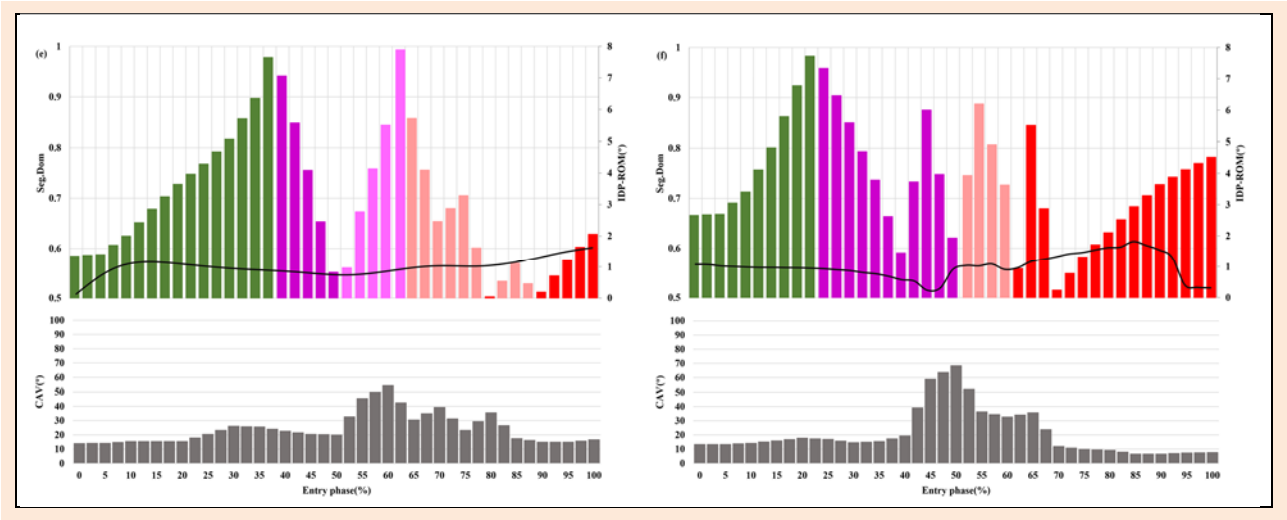

Figure 6. Coupling angle mapping (CAM), segmental dominance (Seg.Dom), Inter-data point range of motion (IDP-ROM) and coupling angle variation (CAV) profiling representing mean elite (e) and sub-elite (f) trunk-thigh coordination during entry phase (See Figure. 3 for colour-scale legend).

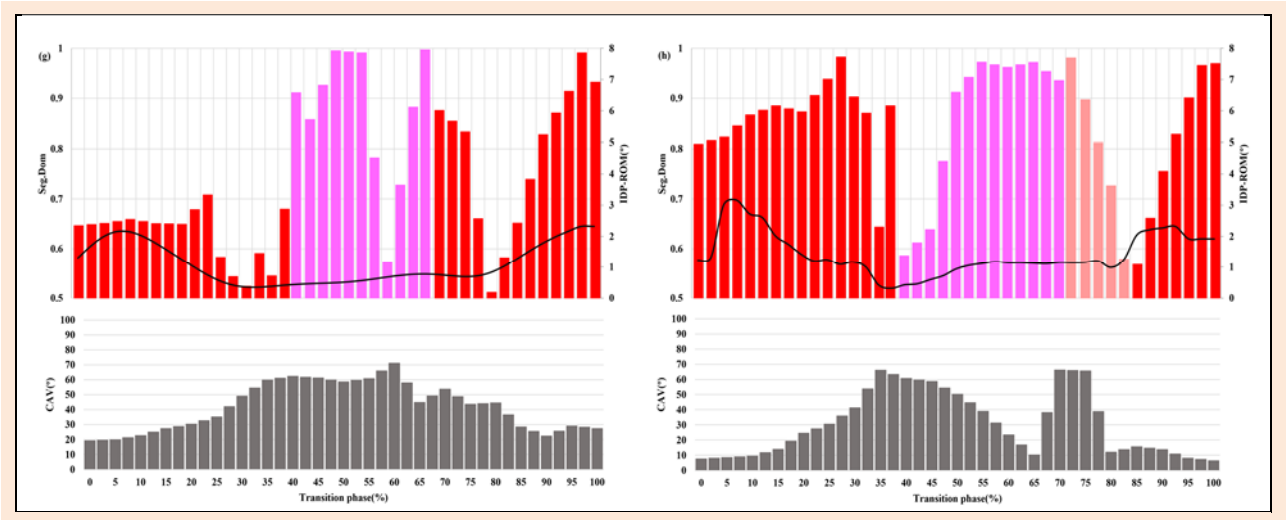

Figure 7. Coupling angle mapping (CAM), segmental dominance (Seg.Dom), Inter-data point range of motion (IDP-ROM) and coupling angle variation (CAV) profiling representing mean elite (g) and sub-elite (h) trunk-thigh coordination during transition phase (See Figure. 3 for colour-scale legend).

Results

Statistical data and time at each phase

The RMSE for the angle measurement during the trial test between auto-tracking and manual operation was 0.52. No significant difference was found between the two methods ($p = 0.59$). The ICC (2,1) for the angle measurement from three experienced researchers was 0.93, CI 95% is [0.9, 0.95] and the p-value is 0.00 with significant high level of inter-operator reliability. The start time of athletes was

shown in Table 2. The results showed no significant difference between the elite and the sub-elite in the total time of the four stages. The time for on-block phase for elite athletes is 0.54 ± 0.04s, which is significantly shorter than that for sub-elite athletes' (0.66 ± 0.09s). In the flight phase and entry phase, there is no significant difference between elite athletes and sub-elite athletes. The time of the transition phase for elite athletes is 0.62 ± 0.30s, significantly longer than that for sub-elite athletes (0.46 ± 0.22s). The time for elite athletes to reach five meters is 1.35 ± 0.17s, which is significantly shorter than the time for sub-elite athletes (1.63 ± 0.14s).

On-block phase

The CAM and CAV for elite athletes and sub-elite athletes on the block phase were shown in Figure 4. Both groups of athletes showed an anti-phase coordination pattern (-/+) in blue bins before the hand off the block but the elite showed more thigh dominance (around 0.7 in average) before 20% of the on-block phase., and sub-elite athletes were dominated by the trunk with dominance rate over 0.8(light blue bins) before 22.5%. Then, both showed the in-phase coordination pattern but in different directions of segment rotation (green vs. red) at hand-off. After the hand left the block, both groups showed an anti-phase coordination pattern (+/-) in purple mainly dominated by leg pushing. The elite athletes showed full thigh dominance (0.98 dominance rate) after the hand-off, while the sub-elite athletes showed the first trunk and then thigh dominance. Around 10% higher CAV was observed in the elite group at 50% of the on-block phase, just prior to back foot take-off. Both groups showed an increase in CAV, with values continuing to rise up to 70% before the hand leaves the block.

Flight phase

The CAM and CAV for elite athletes and sub-elite athletes in the flight phase were shown in Figure 5. In this phase, both athletes showed similar coordination patterns, with the dark purple anti-phase thigh dominant coordination pattern (+/-) shortly appearing first, followed by the in-phase thigh dominant coordination pattern (-/-). However, the anti-phase thigh dominant coordination pattern (+/-) in the sub-elite accounted for longer time domain (90% of flight phase) than the elite (<5%) in the flight phase. The CAV of elite athletes during the first half of flight phase was, on average, up to 20% higher than that of sub-elite athletes.

Entry phase

The elite athletes showed a greater proportion of trunk-dominated coordination patterns during entry phase. the peak CAV in both groups (Figure 6) Approximately occurred at the hip entry point where the in-phase trunk dominant (+/+) coordination pattern (pink bin) both shifted from anti-phase (-/+) purple bins at 65% and 52.5% of the flight time, respectively. The coordination patterns sequence (colour bins sequence) of the two groups during the entry phase were generally the same (Figure 6): Shoulder entry for both groups separated the green (in-phase coordination (-/-) and purple bins (anti-phase coordination (+/-)) and hip entry separated the purple and red bins (in-phase coordination (+/+). However, the elite athletes showed a trunk-dominated anti-phase coordination pattern (+/-) from 53% to 63% before hip entry phase (light purple bin showing the highest dominance rate 0.99), while the sub-elite athletes showed a thigh-dominated (dark purple with 0.88 dominance rate) anti-phase coordination pattern before hip entry.

Transition phase

In-phase coordination (+/+) first made the trunk gradually horizontal after entering the water during transition phase in Figure 7. Both elite athletes and sub-elite athletes initially presented a thigh-dominated in-phase coordination pattern (+/+), then trunk dominated the mid of transition phase moving upwards with anti-phase thigh moving downwards (+/-) for the elite while anti-phase (+/-) plus in-phase (+/+) for the sub-elite. Both were ended with highly thigh-dominated pattern. The CAV of the elite was slightly higher (around 10%) than the sub-elite when the thigh dominated, but the higher CAV was found in sub-elite groups between 70 - 80% time domain where the transition from anti-phase to in-phase trunk dominated coordination patterns. For both groups, the overall CAV was around 50% higher in the mid of the transition phase where the trunk was taking dominance (+/-), compared to the early and later transition phase where the thigh dominated.

Table 2. Time spent at each phase and time to key location.

	Elite (n=10)	SD	sub-elite (n=10)	SD	t	p-value	Effect size (d)
Total time(s)	1.80	0.29	1.77	0.37	0.11	0.91	0.06
On-block phase(s)	0.54	0.04	0.66	0.09	-3.23	<0.01**	0.27
Flight phase(s)	0.27	0.03	0.28	0.05	-0.45	0.66	0.24
Entry phase(s)	0.37	0.03	0.38	0.04	-0.49	0.63	0.13
Transition phase(s)	0.62	0.30	0.46	0.22	2.85	<0.01**	1.24
Time to 5m(s)	1.35	0.17	1.63	0.14	-3.87	<0.01**	2.90

* and **represent a significant difference between Elite and Sub-elite swimmers with $p < 0.05$, $p < 0.01$.

Discussion

This study examined the coordination patterns between the trunk and thigh during the dive start, with a focus on the differences between elite and sub-elite swimmers. Using the visualised coupling angle (CA) method, we compared coordination patterns and variability profiles across different start phases. Key findings indicate that coordination patterns were predominantly in-phase (-/-) or anti-phase (-/+) with thigh dominance, and transitions between these patterns generally occurred between adjacent CA bins. Trunk-dominant patterns were associated with higher coordination variability (CAV) in both groups, although the distribution and timing of these patterns varied between

skill levels. These results provide valuable insights into the movement coordination mechanisms during the dive start, highlighting the role of coordination variability (CAV) in skill-level differences. Our findings suggest that swimmers adopt individualised coordination strategies shaped by their dive-in conditions and technical styles. The contrast in how elite and sub-elite athletes manage these strategies—particularly in trunk involvement and phase-specific variability—is further explored in the following sections.

Time on the different phases

The elite athletes reach the 5m position faster than the sub-elite athletes, but the total time used for on-block, flight, entry and transition showed no significant difference between the elite athletes and the sub-elite athletes in this study. The previous studies on start time found that the shorter on-block phase time can help athletes build a lead quickly(Lyttle and Benjanuvatra, 2005; Matúš et al., 2021; Vilas-Boas et al., 2003). Also, we found that the elite athletes took less time ($p<0.01$) to get off the starting block and into the flight phase but spent more time ($p<0.01$) in the transition phase compared to the sub-elite athletes (Table 2). Short on-block phase for the elite may refer to the strategies of a flat aerial trajectory to travel the maximum distance from the block at the lower velocity aims for a quick entry into the water and earlier stroking. On the other hand, the longer on block phase($p<0.01$) may not necessarily mean a bad strategies because the compromise of long duration on pushing off the block at entry may aim for creating a smaller hole for entering water causing a probably longer (pike) aerial trajectory to encounter aquatic resistance later (Vantorre et al., 2014). This could explain the reason that longer on-block and shorter transition phase for the sub-elite groups.

On-block phase coordination patterns

In on-block phase, the coordination angle mapping (CAM) results (Figure 4) revealed distinct in-phase coordination patterns at the hand-off between elite and sub-elite swimmers. Specifically, elite athletes primarily exhibited an in-phase (-/-) pattern (green bins), while sub-elite swimmers showed a (+/+) pattern (red bins), indicating opposite directions of segmental rotation. The (-/-) pattern observed in elites suggests that both trunk and thigh were rotating downward together, facilitating a forward-leaning posture consistent with a front-weighted track start. In contrast, the (+/+) pattern in sub-elites indicates an upward trunk rotation relative to the thigh, reflecting a rear-weighted track start with a more vertical take-off trajectory.

This distinction in body orientation reflects different center-of-gravity strategies. Elite swimmers' forward-leaning posture is advantageous for initiating horizontal momentum earlier. In contrast, sub-elite swimmers' more upright posture may delay forward acceleration. Previous research by (Vilars-Boas et al., 2000) compared front- and rear-weighted track start techniques and found that, although the rear-weighted start produced greater horizontal impulse, its longer on-block time reduced overall effectiveness. Later findings t(Vilas-Boas et al., 2003) confirmed that the rear-weighted start caused greater horizontal displacement during block exit, but at the cost of longer block phase duration. These results support our observation that elite swimmers, favouring the front-weighted start, exhibited significantly shorter($p<0.01$) on-block times than sub-elite swimmers (Table 2).

Immediately following hand-off (the beginning of the purple bins in Figure 4), swimmers-initiated body extension by pushing off the block, showing an anti-phase coordination pattern (+/-). Here, elite swimmers demonstrated thigh-dominant coordination with a much higher segmental dominance rate (0.99), while sub-elite swimmers displayed trunk-dominant (0.89) patterns. This suggests that elites generated propulsion primarily through leg-driven extension, whereas sub-elites relied more on trunk lift to align the body for flight.

Thigh-dominant force application is advantageous because it produces a stronger push-off and higher start reaction forces (Takeda et al., 2017). Elite athletes thus used their leg power more effectively in the front-weighted start to achieve greater take-off velocity. This strategy enables a shorter block time without sacrificing push-off effectiveness, ultimately contributing to faster times at 5 meters. These findings align with earlier work by Bloom et al. (1978), which emphasized the importance of balancing time spent on the block with sufficient force generation to maximize initial velocity.

With respect to coordination variability, both groups showed higher CAV before the back foot left the block and lower CAV afterward. However, elite athletes exhibited greater pre-takeoff CAV than sub-elites. This may be attributed to more diverse arm swing strategies among the elite group. For example, while some elite swimmers swung their arms forward during the block phase, others used a backward swing known as the Volkov start, which continued into the aerial phase (Seifert et al., 2010b). These variations suggest that, despite similar outcome performance, elite athletes may adopt individualized techniques that introduce variability at specific phases of the start.

Flight phase coordination patterns

Both groups of athletes exhibited similar coordination patterns during the flight phase. Specifically in Figure 5, both showing an anti-phase thigh dominant coordination pattern (+/-) followed by an in-phase thigh dominant pattern (-/-). However, the sub-elite group had a relatively higher rate (Seg.Dom>0.9) of anti-phase thigh dominant coordination pattern (+/-). During this phase, the anti-phase thigh dominant coordination pattern (+/-) indicates the unfolding of the body, while the in-phase thigh dominant pattern (-/-) means that the body gradually dips in the air towards the water. The lower rate of anti-phase thigh dominant coordination pattern (+/-) in elite swimmers, compared to sub-elite swimmers, suggests that the elite swimmers complete their body extension in the air earlier and in a more synchronized manner, allowing them to prepare their entire body posture for entry with greater ease.

Previous studies by Mclean et al.(2000) and Vantorre et al. (2010b) have highlighted the importance of generating sufficient angular momentum for a clean water entry. This requires swimmers to have enough time to rotate while in flight to enter the water through a small

hole(McLean et al., 2000; Vantorre et al., 2010a; Vantorre et al., 2010b). As a result, elite athletes' earlier body extension earlier during the flight phase, enables them to adjust their body posture in the air more efficiently, facilitating an optimal entry position.

Throughout the flight phase, both groups demonstrated a clear thigh-dominated pattern, driven by the angular momentum generated during the on-block phase. The continuous upward lift of the thighs (evident from the decreases thigh angle in Figure 5) helps the athletes gain upward angular momentum and rotate quickly through the air(Bartlett, 2014; Taladriz et al., 2016; Wang et al., 2024). The similar thigh-dominated patterns suggest that both groups of athletes recognise the necessity of quickly positioning their bodies for an optimal water entry.

Notably, elite athletes exhibited a higher coupling angle variation during the flight phase compared to sub-elite swimmers. This greater variability suggests that elite swimmers employ more diverse strategies to adjust their body posture during the flight phase, preparing for a cleaner entry compared to their counterparts.

Entry phase coordination patterns

During the entry phase, swimmers aim to achieve a streamlined body posture by utilizing the angular momentum (Taladriz et al., 2016) generated from the leg drive to facilitate a smooth water entry. Both groups transitioned from the flight phase to the entry phase with an in-phase coordination pattern (-/-) as indicated by the dark green bins in Figure 6, suggesting a coordinated entry movement. Following the shoulder entry, the anti-phase coordination pattern (+/-) gradually shifts the direction of the body movement from downward to forward. This coordination pattern also elevates the legs, creating a better position for entry, allowing the body to enter the water through a small hole. se to entered the water in the dark green bins (in-phase coordination pattern (-/-) from the flight phase to the earlier entry phase, The purple anti-phase coordination pattern (+/-) after shoulder entry gradually changes the direction of the body movement from downward to forward, and this coordination pattern also elevates the leg position to create a better entry position to allow the body to enter the water through a small hole.

Before and after hip entry, the elite athletes demonstrated a greater trunk-dominated coordination. Elite athletes rely on the upward lift of the trunk to gradually and naturally transform the vertical velocity to horizontal after hip entry. In contrast, sub-elite swimmers displayed a more thigh dominant coordination pattern, which primarily assists in changing the body's direction from a downward dive to forward.

The higher dark green bins i.e. Seg.Dom rate (-/-; refer to Figure 3) for the sub-elite in the flight and entry phases (Figure 5. and Figure 6.) indicate an excessive thigh-up (i.e. foot-up) position. This misalignment may cause the body on a back arch, resembling a 'banana shape' before and after hip entry. Such position would increases the swimmer's cross-sectional area in relation to the water, thereby escalating the form drag. (Naemi et al., 2010).

After the hip joint enters the water, the sub-elite athletes exhibited 30% longer in-phase thigh-dominated coordination(+/+) possibly. This may be attributed to the excessive thigh-dominated lift (higher dark green bins) in flight phase and earlier entry phases, which would lead to a leg splash. creating a further wave darg with larger water hole (Godoy-Diana and Thiria, 2018).

Transition phase coordination patterns

During the transition phase, both groups gradually align their bodies parallel to the pool bottom. During this phase, the both groups maintain a coordinated movement pattern characterized by in-phase thigh-dominated coordination (+/+). Elite athletes demonstrate a weaker thigh-dominant coordination pattern, with thigh dominance rate less than 0.75(Needham et al., 2020). This suggests that, during this period, elite athletes have a reduced tendency for thigh segment rotation towards the pool bottom compared to sub-elite athletes. This reduced thigh movement, as reflected in the IDP-ROM (0 - 40%), likely generates less active drag, facilitating smoother transition for the elite.

Sub-elite swimmers, on the other hand, may display a more pronounced downward thigh flapping motion, as indicated by higher IDP-ROM and thigh dominance rate in Figure 7 at the begin of transition phase. After the initial thigh dominance (as observed in the first series of red bins in Figure 7), both groups gradually adjust their bodies to a position parallel to the pool bottom, preparing for upwards and forwards movement due to the 15m allowable distance(van Dijk et al., 2020). This adjustment is accomplished through an anti-phase trunk dominant coordination pattern (+/-) as shown in the light purple bins.

Upon slightly lifting the trunk in preparation for upwards and forwards under water kicking, the swimmers will perform an upbeat kick to initiate the underwater dolphin kick, lifting the shank while pushing down the thigh, thus presenting an in-phase coordination pattern (+/+). Elite swimmers adopt a thigh-dominant coordination pattern during the upbeat kick to initiate the underwater dolphin kick, whereas sub-elite swimmers initially use a trunk dominant coordination pattern to perform the same action.

The initial trunk dominant coordination pattern (+/+) observed in sub-elite swimmers, along with higher IDP-ROM (Figure 7h), results in a greater trunk elevation leading to an increased tendency for upward movement at deep underwater position. This indicates that the trunk dominance to initiate underwater dolphin kicking with higher IDP-ROM may not be an efficient strategy, as the sub-elite swimmers spent longer time in the on-block phase (Table 2.). The compromise of longer time required for higher angular momentum (Taladriz et al., 2016) should have helped the sub-elite swimmers to achieve a better streamlined body position when entering the water (Vantorre et al., 2014). However, the more sudden change of the trunk angle in this phase (pink bins in Figure 7h) at high velocity and deep position can result in significant active and passive drag(Morais et al., 2020; Vennell et al., 2006) ,counteracting the time compromise on block. In contrast, the elite swimmers may approach to the 15-meter mark with a gradual upward movement tendency, supported by a stable trunk with less IDP-ROM during trunk dominating (light purple bars in Figure 7.g) at transition phase. This controlled movement is indicative of elite swimmers'

ability to maintain a more efficient transition.

Elite swimmers adopts different dive start coordination patterns that align with their individual style (Vantorre et al., 2010b). The coupling angle variation (CAV) of elite athletes was found to be higher than that of sub-elite athletes at many time points, suggesting that elite athletes may employ more diverse strategies during dive-in process. Elite swimmers are better able to adjust their body alignment according to their previous dive-in conditions. This previous condition can be viewed as a "constraint" during the dive-in process. This constraint varies between individuals (e.g. travelling more distance in the air or rotating more to enter properly). Ultimately, this variance leads to different approaches by different swimmers, all aimed at minimizing drag and optimizing the trunk lift movement during the transition phase.

Limitations

Several limitations should be considered in this study. First, the sample was composed exclusively of male swimmers, with no female participants included. Previous research has demonstrated sex-based differences in swimming performance and biomechanics(Knechtle et al., 2020), highlighting the need for future studies to include female athletes to better understand potential gender differences in the coordination of swimming starts.

Second, the scope of our analysis was limited to the coordination between the trunk and thigh segments, which we identified as the key body segments for the propulsion phase of the swimming start. While these two segments are crucial in the initiation of movement, the coordination of other segments, such as the arms and calf muscles, also plays a significant role in the overall performance. Therefore, future research should expand the investigation to include additional segmental interactions, particularly between the arms and trunk or between the thighs and calves, to provide a more comprehensive understanding of the coordination patterns involved in the swimming start.

Lastly, the current study did not include samples from top-tier swimmers, such as Olympic medallists, whose coordination patterns during the start could provide valuable insights. The inclusion of such elite swimmers would allow for a more detailed analysis of their unique start coordination, which could offer important training implications for aspiring athletes. Future research should consider incorporating elite-level swimmers to better understand the coordination strategies employed by the world's best performers and how these strategies can inform coaching practices.

Conclusion

The time required to reach a specific distance or phase does not directly indicate a superior dive start, since swimmers must balance drag reduction with rapid entry to initiate stroking. Our findings show that thigh dominance primarily governs the dive-in process across most of the four phases for both elite and sub-elite swimmers. However, the appearance of trunk-dominant patterns in the on-block, entry, and transition phases is associated with higher CAV. Elite swimmers tend to use a more trunk-dominant pattern during the entry phase, enabling a horizontal forward dive-in, while sub-elite swimmers displayed increased trunk dominance in the transition phase. These results highlight the individualised nature of coordination strategies and provide insights for designing tailored training programs that optimize the trade-off between drag reduction and prompt entry.

Acknowledgements

The authors declare that the research was conducted in the absence of any commercial or financial relationships that could be construed as a potential conflict of interest. All authors have no conflict of interest to disclose. This study was sponsored by the Zhejiang Province Science Fund for Distinguished Young Scholars (LR22A020002), Key R&D Program of Zhejiang Province China (2021C03130), Ningbo key R&D Program (2022Z196), the Philosophy and Social Sciences Project of Zhejiang Province, China (22QNYC10ZD, 22NDQN223YB), Ningbo Natural Science Foundation (20221JCGY010532), Zhejiang Xinmiao Talents Program(2023R405088), and Zhejiang Office of Philosophy and Social Science (21NDJC005Z). While the datasets generated and analyzed in this study are not publicly available, they can be obtained from the corresponding author upon reasonable request. All experimental procedures were conducted in compliance with the relevant legal and ethical standards of the country where the study was carried out.

References

Arellano, R., Moreno, F., Martinez, M., and Ona, A. (1996) A device for quantitative measurement of starting time in swimming. *Biomechanics and Medicine in Swimming VII*, 195-200. https://doi.org/10.4324/9780203993354

Bartlett, R. (2014) *Introduction to sports biomechanics: Analysing human movement patterns*. Routledge. https://doi.org/10.4324/9781315889504

Bartlett, R., Wheat, J., and Robins, M. (2007) Is movement variability important for sports biomechanists? *Sports Biomechanics* **6**, 224-243. https://doi.org/10.1080/14763140701322994

Batschelet, E. (1981) *Circular statistics in biology*. Academic Press.

Bloom, J., Hosler, W., and Disch, J. (1978) Differences in flight, reaction and movement time for the grab and conventional starts. *Swimming Technique* **15**, 34-36.

Chollet, D., Chalies, S., and Chatard, J. C. (2000) A new index of coordination for the crawl: Description and usefulness. *International Journal of Sports Medicine* **21**, 54-59. https://doi.org/10.1055/s-2000-8855

Cohen, J. (1988) *Statistical power analysis for the behavioral sciences*. The SAGE Encyclopedia of Research Design, 567. https://doi.org/10.4324/9780203771587

Cossor, J., and Mason, B. (2001) Swim start performances at the Sydney 2000 Olympic Games. In: *ISBS-Conference Proceedings Archive*, 70-74.

Gao, L., Gusztáv, F., and Gao, Z. (2025) Effects of loading positions on lower limb biomechanics during lunge squat in men with different training experience. *Physical Activity and Health* **9**, 198-213. https://doi.org/10.5334/paah.489

Glazier, P. S. (2021) Beyond animated skeletons: How can biomechanical feedback be used to enhance sports performance? *Journal of Biomechanics* **129**, 110686. https://doi.org/10.1016/j.jbiomech.2021.110686

Gleim, G. W., and McHugh, M. P. (1997) Flexibility and its effects on sports injury and performance. *Sports Medicine* **24**, 289-299. https://doi.org/10.2165/00007256-199724050-00001

Godoy-Diana, R., and Thiria, B. (2018) On the diverse roles of fluid dynamic drag in animal swimming and flying. *Journal of the Royal Society Interface* **15**. https://doi.org/10.1098/rsif.2017.0715

Guignard, B., Rouard, A., Chollet, D., Hart, J., Davids, K., and Seifert, L. (2017) Individual-Environment Interactions in Swimming: The Smallest Unit for Analysing the Emergence of Coordination Dynamics in Performance? *Sports Med.* **47**, 1543-1554. https://doi.org/10.1007/s40279-017-0684-4.

Hershler, C., and Milner, M. (1980) Angle-angle diagrams in the assessment of locomotion. *American Journal of Physical Medicine* **59**, 109-125.

Karpiński, J., Rejdych, W., Brzozowska, D., Gołaś, A., Sadowski, W., Swinarew, A. S., Stachura, A., Gupta, S., and Stanula, A. (2020) The effects of a 6-week core exercises on swimming performance of national level swimmers. *PLOS ONE* **15**, e0227394. https://doi.org/10.1371/journal.pone.0227394

Kiuchi, H., Nakashima, M., Cheng, K. B., and Hubbard, M. (2010) Modeling fluid forces in the dive start of competitive swimming. *Journal of Biomechanical Science and Engineering* **5**, 314-328. https://doi.org/10.1299/jbse.5.314

Knechtle, B., Dalamitros, A. A., Barbosa, T. M., Sousa, C. V., Rosemann, T., and Nikolaidis, P. T. (2020) Sex differences in swimming disciplines—can women outperform men in swimming? *International Journal of Environmental Research and Public Health* **17**. https://doi.org/10.3390/ijerph17103651

Lyttle, A., and Benjanuvatra, N. (2005) Start right? A biomechanical review of dive start performance. Zugriff am 15.

Mason, B., Alcock, A., and Fowlie, J. (2007) A kinetic analysis and recommendations for elite swimmers performing the sprint start. In: *ISBS-Conference Proceedings Archive*, 23-27.

Matúš, I., Ružbarský, P., and Vadašová, B. (2021) Key parameters affecting kick start performance in competitive swimming. *International Journal of Environmental Research and Public Health* **18**, 11909. https://doi.org/10.3390/ijerph182211909

McLean, S. P., Holthe, M. J., Vint, P. F., Beckett, K. D., and Hinrichs, R. N. (2000) Addition of an approach to a swimming relay start. *Journal of Applied Biomechanics* **16**, 342-355. https://doi.org/10.1123/jab.16.4.342

Morais, J. E., Sanders, R. H., Papic, C., Barbosa, T. M., and Marinho, D. A. (2020) The influence of the frontal surface area and swim velocity variation in front crawl active drag. *Medicine & Science in Sports & Exercise* **52**, 2357-2364. https://doi.org/10.1249/mss.0000000000002400

Naemi, R., Easson, W. J., and Sanders, R. H. (2010) Hydrodynamic glide efficiency in swimming. *Journal of Science and Medicine in Sport* **13**, 444-451. https://doi.org/10.1016/j.jsams.2009.04.009

Needham, R., Gosling, J., Naemi, R., Hamill, J., and Chockalingam, N. (2018) Coupling angle mapping to assess pelvis-thorax coordination and coordination variability during the maximal instep kick in association football. *ISBS Proceedings Archive* **36**, 602.

Needham, R. A., Naemi, R., and Chockalingam, N. (2015) A new coordination pattern classification to assess gait kinematics when utilising a modified vector coding technique. *Journal of Biomechanics* **48**, 3506-3511. https://doi.org/10.1016/j.jbiomech.2015.07.023

Needham, R. A., Naemi, R., Hamill, J., and Chockalingam, N. (2020) Analysing patterns of coordination and patterns of control using novel data visualisation techniques in vector coding. *Foot (Edinburgh)* **44**, 101678. https://doi.org/10.1016/j.foot.2020.101678

Pau, M., Leban, B., Massa, D., Porta, M., Frau, J., Coghe, G., and Cocco, E. (2022) Inter-joint coordination during gait in people with multiple sclerosis: A focus on the effect of disability. *Multiple Sclerosis and Related Disorders* **60**, 103741. https://doi.org/10.1016/j.msard.2022.103741

Powell, D., Wood, G., Kearney, P., and Payton, C. J. (2021) Skill acquisition practices of coaches on the British Para swimming World Class Programme. *International Journal of Sports Science & Coaching* **16**, 1097-1110. https://doi.org/10.1177/17479541211026248

Seifert, L., Button, C., and Brazier, T. (2010a) *Interacting constraints and inter-limb coordination in swimming*. Routledge. https://doi.org/10.4324/9780203888100

Seifert, L., Delignieres, D., Boulesteix, L., and Chollet, D. (2007) Effect of expertise on butterfly stroke coordination. *Journal of Sports Sciences* **25**, 131-141. https://doi.org/10.1080/02640410600598471

Seifert, L., Leblanc, H., Herault, R., Komar, J., Button, C., and Chollet, D. (2011) Inter-individual variability in the upper-lower limb breaststroke coordination. *Human Movement Science* **30**, 550-565. https://doi.org/10.1016/j.humov.2010.12.003

Seifert, L., Vantorre, J., Lemaitre, F., Chollet, D., Toussaint, H. M., and Vilas-Boas, J. P. (2010b) Different profiles of the aerial start phase in front crawl. *Journal of Strength and Conditioning Research* **24**, 507-516. https://doi.org/10.1519/JSC.0b013e3181c06a0e

Shrout, P. E., and Fleiss, J. L. (1979) Intraclass correlations: uses in assessing rater reliability. *Psychological Bulletin* **86**, 420-428. https://doi.org/10.1037/0033-2909.86.2.420

Slawson, S. E., Conway, P. P., Cossor, J., Chakravorti, N., and West, A. A. (2013) The categorisation of swimming start performance with reference to force generation on the main block and footrest components of the Omega OSB11 start blocks. *Journal of Sports Sciences* **31**, 468-478. https://doi.org/10.1080/02640414.2012.736631

Takeda, T., Sakai, S., Takagi, H., Okuno, K., and Tsubakimoto, S. (2017) Contribution of hand and foot force to take-off velocity for the kick-start in competitive swimming. *Journal of Sports Sciences* **35**, 565-571. https://doi.org/10.1080/02640414.2016.1180417

Takeda, T., Takagi, H., and Tsubakimoto, S. (2012) Effect of inclination and position of new swimming starting block's back plate on track-start performance. *Sports Biomechanics* **11**, 370-381. https://doi.org/10.1080/14763141.2011.637122

Taladriz, S., de la Fuente-Caynzos, B., and Arellano, R. (2016) Analysis of angular momentum effect on swimming kick-start performance. *Journal of Biomechanics* **49**, 1789-1793. https://doi.org/10.1016/j.jbiomech.2016.04.012

Thayer, A., and Hay, J. (1984) Motivating start and turn improvement. *Swimming Technique* **20**, 17-20.

Tor, E., Pease, D. L., and Ball, K. A. (2015) Key parameters of the swimming start and their relationship to start performance. *Journal of Sports Sciences* **33**, 1313-1321. https://doi.org/10.1080/02640414.2014.990486

Trembley, J., and Fielder, G. (2001) Starts, turns and finishes. In: *The Swim Coaching Bible*, 189-206.

Turvey, M. T., Shaw, R. E., and Mace, W. (1978) Issues in the theory of action: Degrees of freedom, coordinative structures and coalitions. In: *Attention and Performance VII*. Routledge, 557-595. https://doi.org/10.4324/9781003310228-35

van Dijk, M.P., Beek, P.J., and van Soest, A.J.K. (2020) Predicting dive start performance from kinematic variables at water entry in (sub-)elite swimmers. *PLOS One* **15**, e0241345. https://doi.org/10.1371/journal.pone.0241345

Vantorre, J., Chollet, D., and Seifert, L. (2014) Biomechanical analysis of the swim-start: a review. *Journal of Sports Science and Medicine* **13**, 223-231.

Vantorre, J., Seifert, L., Fernandes, R.J., Vilas-Boas, J.P., and Chollet, D. (2010a) Biomechanical influence of start technique preference for elite track starters in front crawl. *The Open Sports Sciences Journal* **3**, 137-139. https://doi.org/10.2174/1875399X01003010137

Vantorre, J., Seifert, L., Fernandes, R.J., Vilas-Boas, J.P., and Chollet, D. (2010b) Kinematical profiling of the front crawl start. *International Journal of Sports Medicine* **31**, 16-21. https://doi.org/10.1055/s-0029-1241208

Vennell, R., Pease, D., and Wilson, B. (2006) Wave drag on human swimmers. *Journal of Biomechanics* **39**, 664-671. https://doi.org/10.1016/j.jbiomech.2005.01.023

Vilars-Boas, J.P., Cruz, M.J., Sousa, F., Conceição, F., and Carvalho, M.J. (2000) Integrated kinematic and dynamic analysis of two track-start techniques. In: *ISBS-Conference Proceedings Archive*, 113-117.

Vilas-Boas, J.P., Cruz, J., Sousa, F., Conceicao, F., Fernandes, R., and Carvalho, J. (2003) Biomechanical analysis of ventral swimming starts: comparison of the grab start with two track-start techniques. In: *IXth World Symposium on Biomechanics and Medicine in Swimming*. Saint Etienne: University of Saint Etienne, 249-253.

Wang, M., Song, Y., Zhao, X., Wang, Y., and Zhang, M. (2024) Utilizing anthropometric measurements and 3D scanning for health assessment in clinical practice. *Physical Activity and Health* **8**, 182-196. https://doi.org/10.5334/paah.379

Key points

- Thigh-dominant coordination governs most dive-in phases, while trunk-dominant patterns appear in the on-block, entry, and transition phases and are linked to higher coordination variability.
- Elite swimmers tend to adopt a trunk-dominant pattern during the entry phase, enabling a more horizontal forward dive-in, whereas sub-elites shift trunk dominance to the transition phase.
- Individualized coordination strategies highlight the need for tailored training programs that balance drag reduction with rapid entry, especially for elite swimmers.

AUTHOR BIOGRAPHY

Yi LIN
Employment
Faculty of Sports Science, Ningbo University, Ningbo, China
Degree
MSc Student
Research interests
Biomechanics; swimming; motion analysis; sports science and physical activity.
E-mail: linyi_nbu@hotmail.com

Shudong LI
Employment
Faculty of Sports Science, Ningbo University, Ningbo, China
Degree
PhD
Research interests
Sports training; biomechanics; swimming; sports science and physical activity
E-mail: lishudong@outlook.com

Zhanyi ZHOU
Employment
Faculty of Sports Science, Ningbo University, Ningbo, China
Degree
MSc Student
Research interests
Biomechanics; swimming; motion analysis; sports science and physical activity.
E-mail: zhouzhanyi630@hotmail.com

Luqi YANG
Employment
Faculty of Sports Science, Ningbo University, Ningbo, China
Degree
MSc Student
Research interests
Biomechanics; swimming; motion analysis; sports science and physical activity.
E-mail: yangluqi2022@hotmail.com

Julien S. BAKER
Employment
Department of Sport and Physical Education, Hong Kong Baptist University, Hong Kong, China
Degree
Ph.D. D.Sc. FPhysiol
Research interests
Exercise testing; hypertension; sport biomechanics; exercise physiology
E-mail: jsbaker@hkbu.edu.hk

Yaodong GU
Employment
Faculty of Sports Science, Ningbo University, Ningbo, China
Degree
PhD; Professor (Full)
Research interests
Biomechanics; gait; kinematics; motion analysis
E-mail: guyaodong@nbu.edu.cn

✉ **Shudong Li**
Faculty of Sports Science, Ningbo University, Ningbo, China

✉ **Yaodong Gu**
Faculty of Sports Science, Ningbo University, Ningbo, China